Virology 534 (2019) 54–63

Contents lists available at ScienceDirect

Virology

journal homepage: www.elsevier.com/locate/virology

Targeting the proviral host kinase, FAK, limits influenza a virus pathogenesis and NFkB-regulated pro-inflammatory responses

Silke Bergmann, Husni Elbahesh*,[1]

Department of Microbiology, Immunology and Biochemistry, University of Tennessee Health Science Center, Memphis, TN, 38163, USA

A B S T R A C T

Influenza A virus (IAV) infections result in ~500,000 global deaths annually. Host kinases link multiple signaling pathways at various stages of infection and are attractive therapeutic target. Focal adhesion kinase (FAK), a non-receptor tyrosine kinase, regulates several cellular processes including NFkB and antiviral responses. We investigated how FAK kinase activity regulates IAV pathogenesis. Using a severe infection model, we infected IAV-susceptible DBA/2 J mice with a lethal dose of H1N1 IAV. We observed reduced viral load and pro-inflammatory cytokines, delayed mortality, and increased survival in FAK inhibitor (Y15) treated mice. In vitro IAV-induced NFkB-promoter activity was reduced by Y15 or a dominant negative kinase-dead FAK mutant (FAK-KD) independently of the viral immune modulator, NS1. Finally, we observed reduced IAV-induced nuclear localization of NFkB in FAK-KD expressing cells. Our data suggest a novel mechanism where IAV hijacks FAK to promote viral replication and limit its ability to contribute to innate immune responses.

1. Introduction

Influenza A viruses (IAVs) are major human respiratory pathogens which present a significant public health threat and are responsible for multiple pandemics (1918, 1957, 1968 and 2009) and yearly epidemics that cause more than 500,000 annual deaths globally (Taubenberger and Morens, 2008). IAV infections are typically mild in otherwise healthy individuals; exceptions being sporadic highly-pathogenic avian influenza virus infections (e.g. H5N1 and H7N9). However, seasonal H3N2 and H1N1 IAV infections can still present significant clinical challenges especially in high-risk patients such as children, elderly and immuno-compromised. The disease progression in severe cases is accelerated where the time of symptom onset to requirement of ventilator support is ~3 days. Treatment options are limited relying mostly on antiviral neuraminidase inhibitors (NAIs) and critical care support (Zambon, 2014). Moreover, patients with severe infections often die if they do not receive antivirals like NAIs within 24 h after hospitalization (Randolph et al., 2011; Uchimura et al., 2012). The main focus of antiviral therapy is to prevent or limit damage of the lung epithelium mediated by overly robust immune responses. Unfortunately, NAIs have not been effective in severe H7N9 or H5N1 infections with evidence of antiviral resistance even in seasonal strains highlighting their vulnerability to virus adaptation (Chan et al., 2012; de Jong et al., 2005; Hu et al., 2013). Host targeted antivirals do not suffer from this limitation and current approaches to utilize this approach are under investigation (Elbahesh et al., 2019).

Like most viruses, influenza viruses are dependent on host-factors at every stage of the infection cycle. Viral ribonucleoproteins (vRNPs) are shuttled to the nucleus following entry where each viral genomic segment serves as a template to generate viral mRNAs that encode the viral proteins. Shortly following infection, an arms-race ensues between the host and virus. One of the most important viral proteins is the viral non-structural 1 (NS1) protein which acts as a multifaceted immune modulator to counteract host defenses at various stages of the infection cycle (Ayllon and Garcia-Sastre, 2015; Krug, 2015). Although NS1 mediates antiviral/inflammatory response evasion, IAV infection still activates the NFkB pathway through complex and multilayered signaling cascades. Initial activation of RIG-I by viral RNA triggers downstream activation of MAVS (mitochondrial antiviral-signaling protein) and IKK complexes (IKKα, IKKβ and NEMO) (Hou et al., 2011; Peisley et al., 2013, 2014). The ultimate function of NFkB during IAV infection is controversial. Several studies have shown pro-viral effects of NFkB activation while others have reported that NFkB activation during IAV infection leads to upregulation of antiviral effectors and expression of pro-inflammatory chemokines/cytokines (Goulet et al., 2013; Maelfait et al., 2012; Nimmerjahn et al., 2004; Wurzer et al., 2004; Pauli et al., 2008; Wei et al., 2006; Wang et al., 2000).

The multiple signaling pathways triggered and suppressed by IAVs are typically linked by host kinases (Meineke et al., 2019). Accordingly, phosphorylation of several IAV proteins has been shown to regulate the

* Corresponding author.
E-mail address: husni.elbahesh@tiho-hannover.de (H. Elbahesh).
[1] Present Address: Research Center for Emerging Infections and Zoonosis (RIZ) University of Veterinary Medicine Hannover Bünteweg 17, 30559, Hannover, Germany.

https://doi.org/10.1016/j.virol.2019.05.020
Received 15 February 2019; Received in revised form 29 May 2019; Accepted 30 May 2019
Available online 01 June 2019
0042-6822/

viral cycle by either promoting replication or evading/suppressing innate immune responses (Hutchinson et al., 2012; Wang et al., 2013; Hsiang et al., 2012; Arrese and Portela, 1996; Mitzner et al., 2009; Zheng et al., 2015). Moreover, several processes are affected by kinase inhibitors including IAV RNA/protein synthesis, cytoplasmic/nuclear shuttling of viral proteins and virion release (Kumar et al., 2011a, 2011b; Pleschka et al., 2001; Kurokawa et al., 1990; Root et al., 2000). Focal adhesion kinase (FAK) is a non-receptor tyrosine kinase. Originally identified in focal adhesion complexes (FA) that tether the actin cytoskeleton to the extracellular matrix; cytoplasmic and nuclear fractions have been identified (Schaller, 2010; Lim et al., 2008). FAK-Y397 phosphorylation provides a binding site for Src kinases and PLCγ that then phosphorylate FAK-Y576/577 and several other residues for maximal activation (Schaller, 2010; Calalb et al., 1995). FAK scaffolding and kinase activities regulate actin reorganization in migration and receptor endocytosis, embryonic development and expression of several cellular proteins (Schaller, 2010; Calalb et al., 1995; Cicchini et al., 2008; Lim et al., 2012). FAK regulates in vivo functions of T cells, B cells and macrophages (Chapman et al., 2013; St-Pierre and Ostergaard, 2013; Park et al., 2013) thereby modulating the cellular immune response. FAK is also a component of the intracellular RIG-I-Like receptor antiviral pathway (Bozym et al., 2012). Our previous in vitro studies showed that FAK activity promotes efficient entry and replication of several IAV strains from different subtypes (Elbahesh et al., 2014, 2016). Others have also reported roles for FAK during other viral infections (Cheshenko et al., 2005; Kaminsky et al., 2012; Krishnan et al., 2006; Bouchard et al., 2006; Fouquet et al., 2015; Ni et al., 2015). We investigated the contribution of FAK kinase-activity to IAV pathogenesis and innate immune responses during a severe IAV infection.

2. Results

2.1. Short-term inhibition of in vivo FAK kinase activity prolongs survival

We used a well-established and validated small-molecule FAK inhibitor (Y15) to inhibit FAK-pY397 and subsequent FAK activation (O'Brien et al., 2014; Golubovskaya et al., 2008; Golubovskaya et al., 2015; Golubovskaya et al., 2012; Hochwald et al., 2009). We previously showed that inhibiting FAK kinase-activity by either Y15-treatments or expression of a kinase-dead mutant results in reduced IAV entry and polymerase activity in transformed and primary human lung cells (Elbahesh et al., 2014, 2016). Y15 was shown by others to inhibit FAK activity in vitro and in vivo, but not other related tyrosine kinases (Schaller, 2010; Calalb et al., 1995; Cicchini et al., 2008; Lim et al., 2012; Chapman et al., 2013; St-Pierre and Ostergaard, 2013; Park et al., 2013; Lee et al., 2012; Zhang et al., 2016). We validated Y15-specificity against FAK using in vitro kinase assays and found that even at a relatively high in vitro concentration (2.5 μM), there was minimal effects on 7 related kinases, including those reported to play a role in IAV infection [Fig. 1A]. We next established a non-toxic dose of FAK inhibitor I (Y15) by comparing 3 doses (5, 10 and 15 mg/kg diluted in 10% DMSO/PBS) administered intranasally in 20 μl daily for 3 days using IAV-susceptible DBA/2 J (D2) mice. In contrast to published data using different mouse strains (Golubovskaya et al., 2012, 2015), we found that only the 5 mg/kg dose did not lead to weight-loss compared to 10 and 15 mg/kg doses (> 10% weight-loss that lasted until day 5) [Fig. 1B].

D2 mice exhibit extremely accelerated IAV replication and earlier onset of severe inflammatory responses than more resistant mouse strains like Balb/c and C57BL/6. This progression in severity is also observed in human patients with severe IAV infections (Randolph et al., 2011; Uchimura et al., 2012); therefore, D2 mice represent a clinically relevant mouse model. We examined the impact of inhibiting FAK kinase-activity on IAV pathogenesis using a severe model of infection (Dengler et al., 2012, 2014; DesRochers et al., 2016; Shin et al., 2015; Srivastava et al., 2009). D2 mice were intranasally inoculated with 5 mg/kg Y15 in 20 μl once daily at days −1, 0, 1 of infection [Fig. 2A]; on day 0 (day of infection), mice were inoculated with Y15 and infected 6 h later with 50 PFU of H1N1 IAV (PR8). Although weight-loss was similar in both infected groups [Fig. 2B], three doses of Y15 were sufficient to significantly extend survival time by 3 days and increase survival [Fig. 2C]. Importantly, DMSO-treated mice either succumbed to the infection (4/8) or were euthanized based on reaching symptom end-points before reaching body weight-loss cut-off. In contrast, most (7/8) Y15-treated mice were euthanized due to reaching body weight-loss cut-off with mild symptoms being observed. Our data indicate that short-term prophylactic intranasal administration of Y15 results in prolonged survival of an extremely susceptible host.

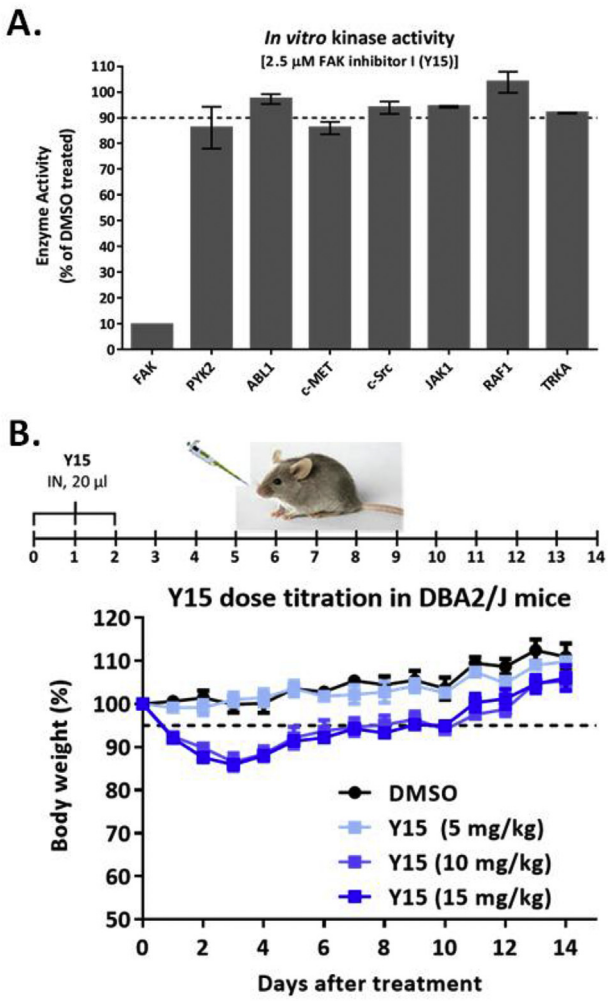

Fig. 1. In vitro specificity and in vivo tolerance of FAK inhibitor (Y15). (A) In vitro kinase activity assays on indicated kinases were carried out using 2.5 μM of Y15 and 10 μM ^{33}p-γATP. Poly(YE) peptide was used as substrate and enzyme activity was measured and compared to DMSO treated samples for each enzyme; error bars are Mean ± SD (n = 2). (B) Y15 toxicity was assessed 10 week old female DBA/2 J mice (n = 3/group) were anesthetized and intranasally inoculated once daily for 3 days with Y15 in 10% DMSO-PBS at 5, 10 or 15 mg/kg in 20 μl (10 μl per nare). Body weight-loss and behavior was monitored for 14 days. Control mice were inoculated with 10% DMSO-PBS.

2.2. Short-term Y15 treatment limits in vivo viral replication and pathogenesis

To determine the effect of inhibiting FAK kinase activity on viral load, we compared viral load in nasal turbinate, trachea and lungs of DMSO treated and Y15-treated mice; at 3 and 5 days post-infection

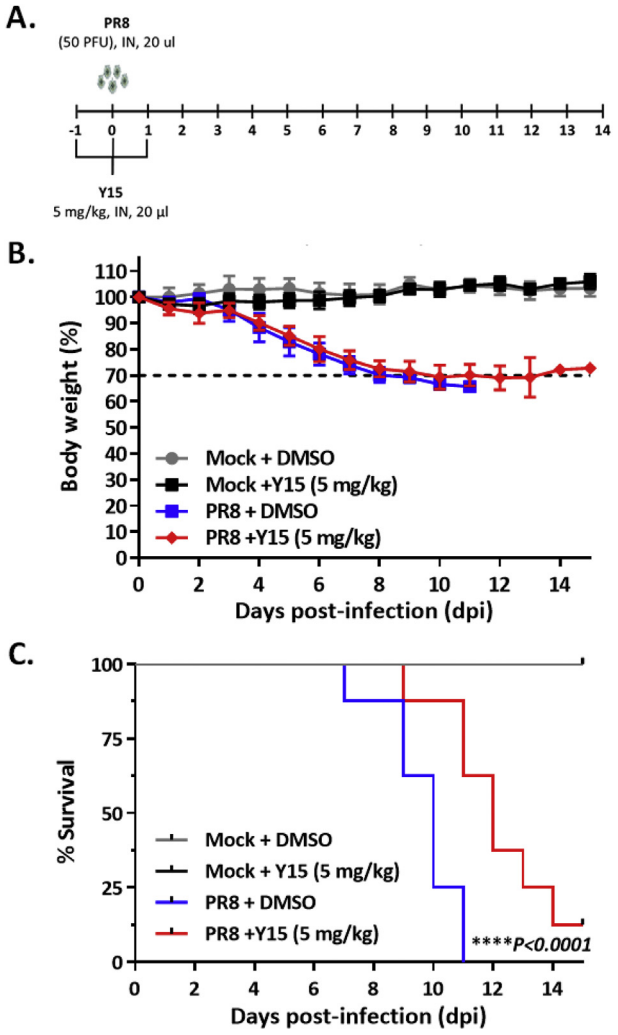

Fig. 2. Effect of short-term Y15 on IAV induced mortality and morbidity. (A to C) 10–12 week old female mice (n = 8/group) were intranasally infected with IAV (PR8 50 pfu in 20 µl). Mice were intranasally inoculated once daily for 3 days with Y15 (5 mg/kg in 10% DMSO-PBS) in 20 µl (10 µl per nare) on −1, 0, and 1 dpi. Control mice were inoculated with 10% DMSO-PBS and either mock or IAV-infected. Body weight-loss (B) and survival (C) was monitored daily for 14 days. Mantel-Cox Log-rank test was used to determine statistical significance for survival curves; $^{****}p < 0.0001$.

(dpi) tissues were harvested and homogenized for viral load quantification [Fig. 3A]. Although there was no difference in viral load at 3 dpi between Y15-treated and DMSO-treated mice in any of the tissues (data not shown), Y15 treatment led to a significant decrease (> 1 $\log_{10}$) in viral load at 5 dpi in both trachea (57-fold) and lungs (13.6-fold) compared to DMSO-treated mice [Fig. 3B]. Immune-cell infiltration into the lungs serves to limit virus spread but can also lead to damage of the lung-epithelium resulting in increased morbidity and/or mortality. Histochemistry staining showed a significant reduction (~59%) of cellular infiltration into the broncho-alveolar space at 5 dpi in Y15-treated mice compared to DMSO-treated mice [Fig. 3C]; suggesting that inhibition of FAK kinase activity not only limits viral replication but also cell-mediated immune responses. This reduction in cellular infiltration could lead to reduced tissue damage and disease burden which likely contributes to the prolonged survival and reduced symptoms of Y15-treated mice compared to DMSO-treated mice.

2.3. Reduced IAV-induced pro-inflammatory cytokines in Y15 treated mice

We next compared the levels of chemokines/cytokines in bronchoalveolar lavage (BAL) fluid at 3 and 5 dpi in Y15-treated and DMSO-treated mice. We observed significantly reduced induction of several pro-inflammatory chemokines/cytokines (G-CSF, IFN-g, KC, IL-6, MIG, MIP-2a and IP-10) at 3 dpi and at 5 dpi (IL-1b and IP-10) in Y15-treated mice [Fig. 4A]. Interestingly, we observed a significant increase from 3 to 5 dpi in Eotaxin, G-CSF and IL-1b in both Y15-and DMSO-treated mice [Fig. 4B and C]. However, while there was a decrease in MIP-1a, MIP-2, Rantes and VEGF in BAL from DMSO treated mice [Fig. 4B], there was a significant increase in LIF and a minimal increase in MCP-1 in BAL from Y15-treated mice during the same time (3 vs 5 dpi) [Fig. 4C]. These kinetics indicate that FAK-dependent differential regulation of IAV-induced pro-inflammatory responses is observed earlier than differences in lung viral load (3 dpi vs 5 dpi), suggesting that viral load differences are not driving the observed differences in BAL chemokine/cytokine in DMSO vs Y15-treated mice. G-CSF, IFN-g, KC, IL-6, MIG, MIP-2a and IP-10 all regulate early neutrophil and macrophage infiltration to the site of infection and subsequent infiltration by cytotoxic T lymphocytes (CTLs) and natural killer (NK) cells. The reduction of these cytokines in Y15 treated mice could result in reduced damage to the epithelium by the cellular response that could lessen disease burden.

To confirm the effect of Y15 on IAV replication at the epithelial cell-layer in the absence of infiltrating immune cells, we used ex vivo precision-cut lung slices (PCLS) generated from uninfected D2 mouse lungs. PCLS were infected with PR8 at 10^4 PFU ± DMSO or Y15 for 48 h. Culture supernatant was collected at 0.5, 8, 24 and 48 hpi and viral titers quantified. We observed a ~21-fold reduction by 8 hpi and ~67-fold reduction by 24 hpi in virus titers in Y15-treated IAV-infected PCLS [Fig. 5] indicating that Y15-treatment results in epithelial-cell specific reduction in viral load; consistent with our previously published results using human tissue culture systems and multiple IAV strains (Elbahesh et al., 2014, 2016).

2.4. FAK kinase activity regulates in vitro IAV induced NFkB-activation

As we observed a significant reduction in several IAV induced pro-inflammatory cytokines that are regulated by NFkB in Y15-treated mice, we next determined the effect of inhibiting FAK kinase activity in vitro using A549 cells (A549-NFkB) stably expressing a secreted alkaline phosphatase reporter under control of NFkB promoter (NFkB-SEAP). A549-NFkB cells were infected with PR8 at a moi of 5 and at 5 hpi the cells were treated with Y15 (25 µM). NFkB activation was quantified by measuring SEAP activity in culture supernatant collected at 12, 24, 36 and 48 hpi. We observed a subtle but significant decrease in NFkB-SEAP activity at 24 hpi in Y15-treated cells compared to DMSO-treated cells with differences increasing in magnitude [Fig. 6A]. Interestingly, this effect of Y15 on NFkB activation was dependent on the moi used as we did not detect a significant difference using a lower moi (0.5) [Fig. 6B]. We previous demonstrated that efficient IAV entry and RNA replication require FAK kinase activity. However, FAK chemical inhibition is rarely complete; therefore, it is likely that at higher moi infections the pool of “activatable ” FAK is in limiting concentrations. Whereas in low moi infections “activatable” FAK is in excess amounts during early points.

2.5. FAK-dependent NF_kB regulation is independent of IAV NS1

Considering NS1 regulates NFkB activation through multiple mechanisms, we aimed to determine if the observed FAK dependency of NFkB activation requires NS1. We initially compared NFkB activation in A549-NFkB cells infected with the pandemic H1N1 IAV strain (A/California/04/2009; CA/04) at a moi of 5. Similarly to what was observed for the laboratory strain PR8, NFkB activation was significantly limited in Y15-treated cells compared to the DMSO treated cells [Fig. 7A]; indicating that our observations are not strain specific. To dissect the role of FAK kinase activity in the absence of the effects on

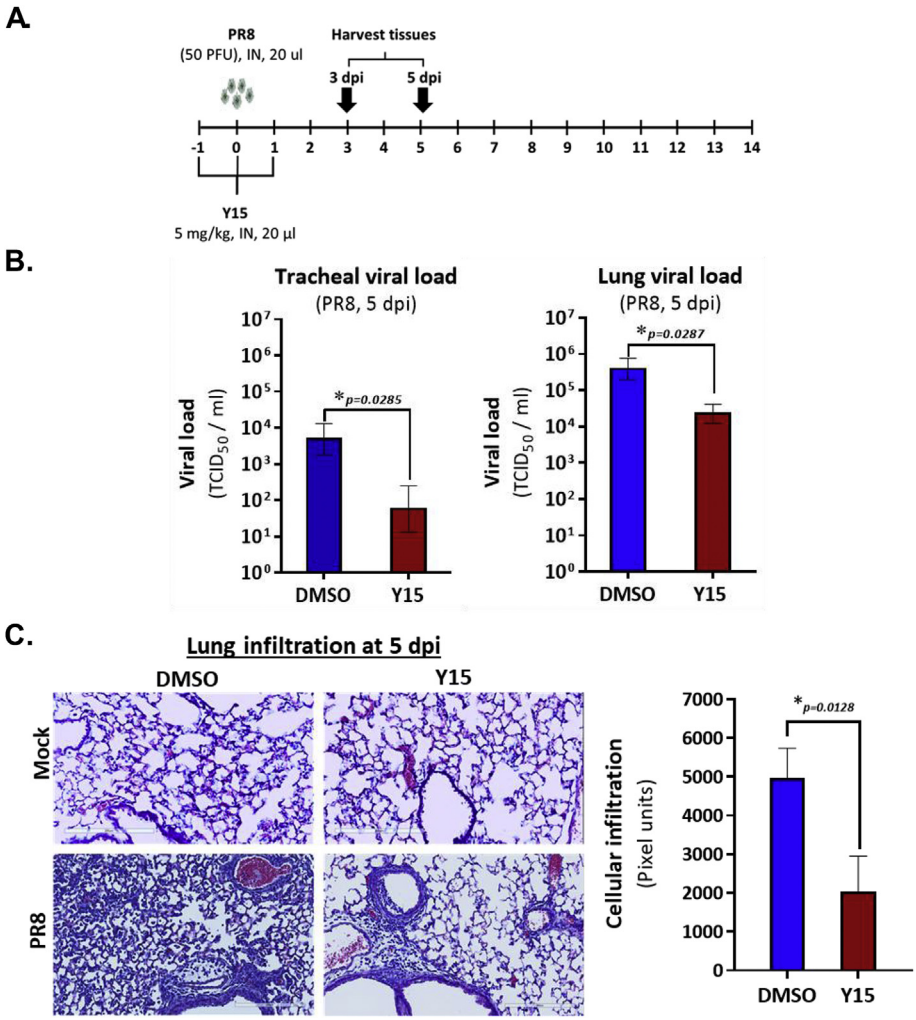

Fig. 3. Effect of short-term Y15 on viral replication in vivo. (A to C) 10–12 week old female mice (n = 4/group; from two independent experiments) were intranasally infected with IAV (PR8 50 pfu in 20 µl). Mice were intranasally inoculated once daily for 3 days with Y15 (5 mg/kg in 10% DMSO) or DMSO in 20 µl (10 µl per nare) on −1, 0, and 1 dpi. Control mice were inoculated with DMSO in PBS and either mock or IAV-infected. (B) Trachea and lungs from DMSO or Y15-treated IAV-infected mice were isolated at 5 dpi and infectious viral load was determined by $TCID_{50}$ method. (C) Lungs were isolated at 5 dpi from mock or IAV infected mice that were either DMSO or Y15 treated and analyzed by H&E staining; representative images are shown. Cellular infiltration was quantified using ImageJ particle measurement analysis (3 images/group). Particles were counted if they contained 3 or more pixels. Unpaired, nonparametric Mann-Whiteny *U*-test was used to determine statistical significance with indicated *p* values.

viral entry, we utilized the minigenome assay to assess NFkB activation and viral polymerase activity in A549 cells overexpressing wild-type FAK (A549-FAK-WT) or a kinase-dead dominant negative FAK mutant (A549-FAK-KD). Cells were transfected with dual promoter plasmids encoding the PA, PB1, PB2 and NP viral proteins; cells were also transfected with pPOLI-358-FFLuc (polymerase activity reporter), NFkB-SEAP, and control β-galactosidase-expressing pCMV-βgal plasmid for transfection normalization. In the indicated samples a plasmid encoding the viral NS1 protein was also included in the transfection (+NS1). As a positive control for NFkB activation, cells were transfected with the synthetic dsRNA poly(I:C) (2 µg/ml) at 6 hpt (+pIC). At 24 hpt, NFkB-SEAP activity in culture supernatant was measured [Fig. 7B]. To quantify polymerase activity, cells were harvested and firefly luciferase activity was measured and normalized to β-galactosidase activity [Fig. 7C]. We observed a significant reduction in NFkB activity, as well as polymerase activity, in A549-FAK-KD cells compared to A549-FAK-WT cells under all tested conditions. Interestingly, NFkB activation was similar ± NS1 while polymerase activity was ~5-fold higher in cells expressing NS1 [Fig. 7B and C, respectively]. Moreover, poly(I:C) treatment robustly induced NFkB-activation and to a lesser extent in the presence of NS1; however, FAK-KD expression resulted in reduced activation in both cases. Together, our data indicate that FAK kinase activity regulates IAV-induced NFkB activation independently of NS1.

2.6. FAK kinase activity regulates NFkB localization during IAV infection

NFkB activation leads to its translocation to the nucleus where it mediates expression of inflammatory and antiviral genes. We next determined if FAK kinase activity affected NFkB nuclear translocation during IAV infection. A549-FAK-WT and A549-FAK-KD cells were infected with PR8 at a moi 5. At 24 hpi, cells were fixed and permeabilized then immunostained to detect NFkB localization (NFkB) and IAV-infected cells (NP). Minimal nuclear localization of NFkB could be detected in IAV-infected A549-FAK-KD cells, whereas nuclear NFkB could be readily detected in most infected A549-FAK-WT cells [Fig. 8]. This data suggest that FAK kinase activity is required for IAV-induced NFkB nuclear localization and provides further evidence of FAK regulated NFkB signaling during IAV infections.

3. Discussion

Influenza A viruses activate a myriad of signaling pathways at all points of the infection cycle to promote efficient replication. Depending on the timing of the activation events, these signaling cascades may serve anti- or pro-viral functions. The current study expands on our previous reports on the important role FAK plays during in vitro IAV entry and replication of several strains/subtypes (Elbahesh et al., 2014, 2016). Here, we used a highly susceptible mouse strain to model severe IAV infections and we showed that inhibiting FAK kinase activity delayed mortality, increased survival, reduced viral loads and pro-inflammatory immune responses. To our knowledge, this is the first

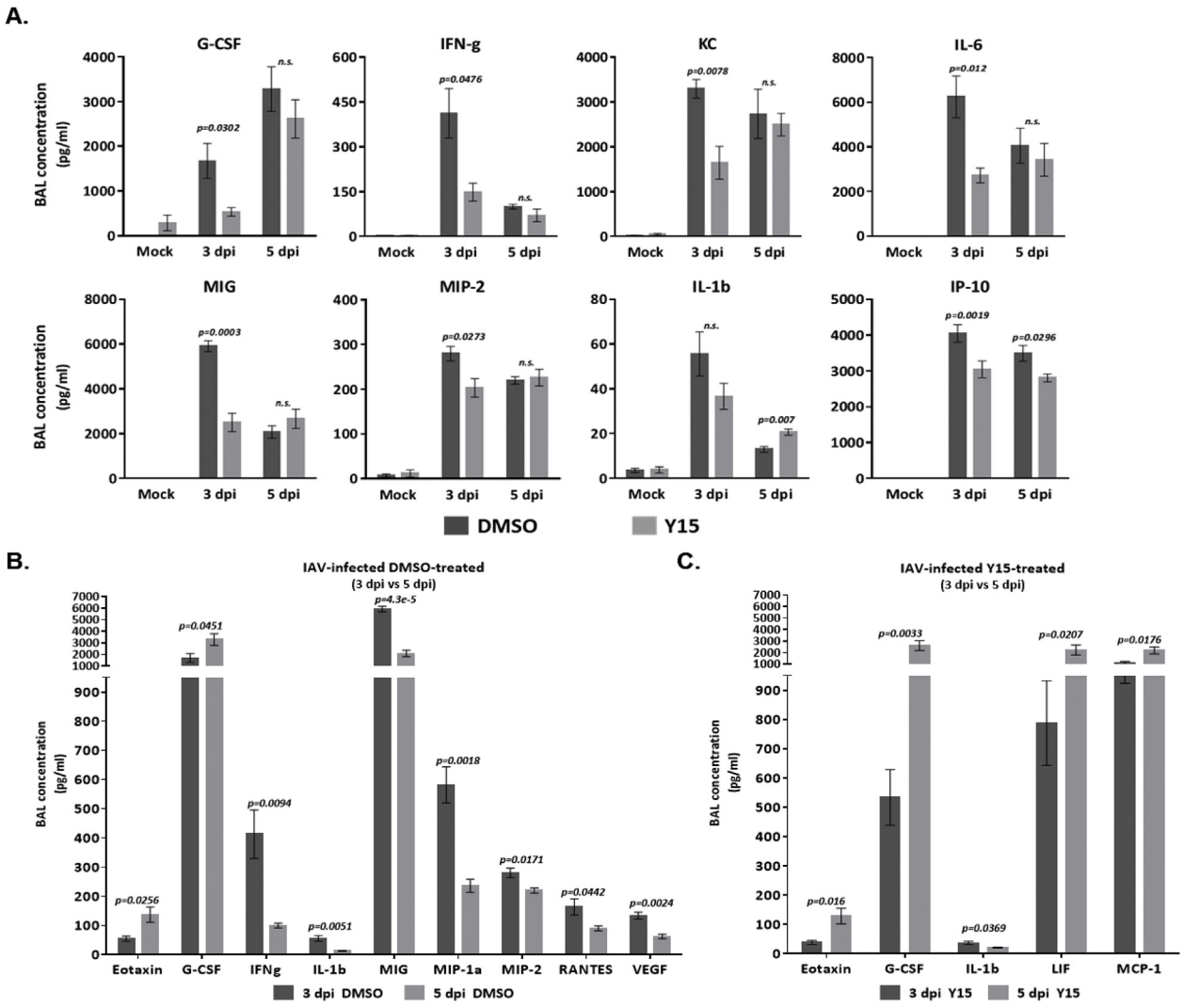

Fig. 4. Effect of short-term Y15 on in vivo proinflammatory chemokine/cytokine induction. (A to C) 10–12 week old female mice (n = 4/group; from two independent experiments) were intranasally infected with IAV (PR8 50 pfu in 20 µl). Mice were intranasally inoculated once daily for 3 days with Y15 (5 mg/kg) or DMSO in 20 µl (10 µl per nare) on −1, 0, and 1 dpi. Control mice were inoculated with DMSO in PBS and either mock or IAV-infected. (A) Statistically significant differences in indicated BAL cytokines/chemokines from IAV-infected DMSO treated (B) or (C) Y15-treated mice are shown. Unpaired, *t*-Test was used to determine statistical significance with indicated *p* values.

demonstration of FAK-mediated regulation of an in vivo viral infection. Furthermore, our complimentary approaches using either specific FAK kinase activity inhibitor (Y15) or a kinase-dead dominant-negative FAK mutant clearly implicate FAK activity is required for efficient NFkB signaling in vitro in the context of IAV infections.

Cellular responses contribute to the IAV-susceptible phenotype observed later during infection in IAV-susceptible DBA/2 J (D2) mice. Compared to IAV-resistant C57BL/6 (B6) mice, D2 mice support > 100-fold higher lung viral loads within the first 24 h which are maintained throughout the infection making D2 mice an ideal model of acute severe IAV infections (Srivastava et al., 2009). We found that short-term (3 daily doses) inhibition of FAK activation was sufficient to reduce tracheal and lung viral loads. Importantly, these reductions were much more robust than those previously reported by others following 8 daily doses of the FDA-approved antiviral Oseltamivir in the same mouse strain (Kim et al., 2013). Given the low infectious dose of our experiments (50 pfu), it is not surprising that viral load differences were not observed until later time-points. We believe that this is in-line with host-factors needed for efficient replication becoming increasingly limited by increasing amounts of replicating virus. Under these conditions, incomplete inhibition/knockdown/inactivation of these host-factors is likely to have the greatest effect at later time points.

In terms of the consequences of increased viral replication in D2 mice, Boon et al. found a significant association between IAV viral loads and chemokine/cytokine mRNAs and that there was no difference in the cytokine/viral RNA ratio between resistant and susceptible mouse strains; suggesting that replication dynamics as the primary drivers of IAV susceptibility (Boon et al., 2009). Interestingly, we observed reductions in viral loads that were at later time points (5 dpi) than reductions in pro-inflammatory cytokines (3 dpi). Although we cannot argue against the impact of viral RNA replication on the induction of inflammatory chemokines/cytokines, our observed kinetics argue against a causal relationship between the two events in response to FAK inhibition and support distinct roles for FAK in viral replication and induction of pro-inflammatory responses. Consistent with the reduction of pro-inflammatory cytokines (G-CSF, IFN-g, KC, IL-6, MIG, MIP-2a and IP-10), we observed reduced immune effector cell infiltration in Y15 treated mice by 5 dpi. This is likely to limit damage to the lung epithelium and subsequent disease burden. Although this reduction in immune response had a limited effect on weight-loss and survival, it is consistent with a recent report indicating that even expression of a functional Mx1 (confers resistance to IAV) is not sufficient to overcome

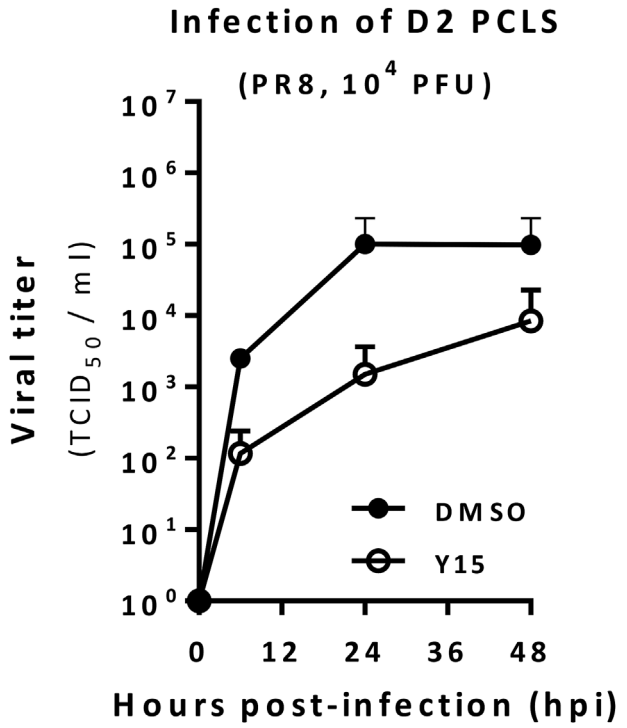

Fig. 5. Effect of Y15 on IAV replication in PCLS. Lungs from three 10–12 week old female D2 mice were harvested and used to generate 300 μm thick precision cut lung slices (PCLS). PCLS were either treated with DMSO or Y15 (25 μM) for 24 h then infected with PR8 (10^4 PFU). DMSO or Y15 were included throughout infection and supernatants were collected at indicated times (n = 3/time-point/treatment) and virus titers were determined by $TCID_{50}$ method. Error bars indicate standard deviation (SD).

a severe infection in D2 mice (Shin et al., 2015). In that study, authors suggested that expression of the Mx1 gene at 3 dpi was still too late to protect D2 mice. Moreover, they also observed a lethal outcome in D2 mice compared to recovery in C57BL/6 mice despite similar proinflammatory cytokines at 5 dpi. We observed reduced disease burden in Y15 treated mice; most of which were euthanized due to reaching weight-loss cut-off. In contrast, DMSO treated mice either succumbed to infection (4/8) or were euthanized due to severe symptoms. It is likely that more drastic differences in survival and weight-loss would be observed if Y15 was more frequently administered (8 vs 3 daily doses) as was previously described using Oseltamivir (Kim et al., 2013). Our PCLS results suggest that Y15 treatment reduces viral replication at the epithelial cell layer even in the absence of infiltrating immune cells. However, this cannot rule out the effect of FAK inhibition on immune cell responses during in vivo IAV infections. Indeed, the source of BAL chemokines/cytokines is not experimentally clear and it is reasonable to assume that epithelial cells and infiltrating immune cells contribute to the milieu of chemokines/cytokines detected.

FAK has recently emerged as a regulator of multiple steps during viral infections. It regulates entry (herpes simplex virus and Kaposi's sarcoma-associated herpes virus) (Cheshenko et al., 2005; Krishnan et al., 2006), replication (hepatitis B virus, murine polyomavirus, rabies virus, and porcine reproductive and respiratory syndrome virus) (Bouchard et al., 2006; Fouquet et al., 2015; Ni et al., 2015; O'Hara and Garcea, 2016), and is involved in transformation by bovine papillomavirus 1 E6 (Brimer et al., 2014) and transduction by adeno-associated virus (Kaminsky et al., 2012). Whereas these studies highlight a proviral role for FAK, two recent studies suggested that FAK can also mediate antiviral responses to several viruses (Bozym et al., 2012; Tian et al., 2015). In those studies they reported that FAK promotes kinase-independent MAVS-signaling and suppression of FAK repressed Interferon-stimulated genes (ISGs) results in increased replication of several viruses (Bozym et al., 2012; Tian et al., 2015). This is in stark contrast to data provided in this study and our published data indicating that FAK kinase-activity serves a proviral role in IAV replication in vitro and in vivo. Although we cannot discount the kinase-independent contribution of FAK to the innate-immune response, it is highly unlikely that limiting induction of ISGs as reported by the other groups would reduce IAV replication.

Influenza A virus infections, like those by most viruses, typically illicit an antiviral response that is mediated in part by NFkB. Interestingly, FAK was recently reported to directly phosphorylate IKKα thereby regulating canonical and non-canonical NFkB pathways and may regulate antiviral and pro-inflammatory responses to IAV (Dwyer

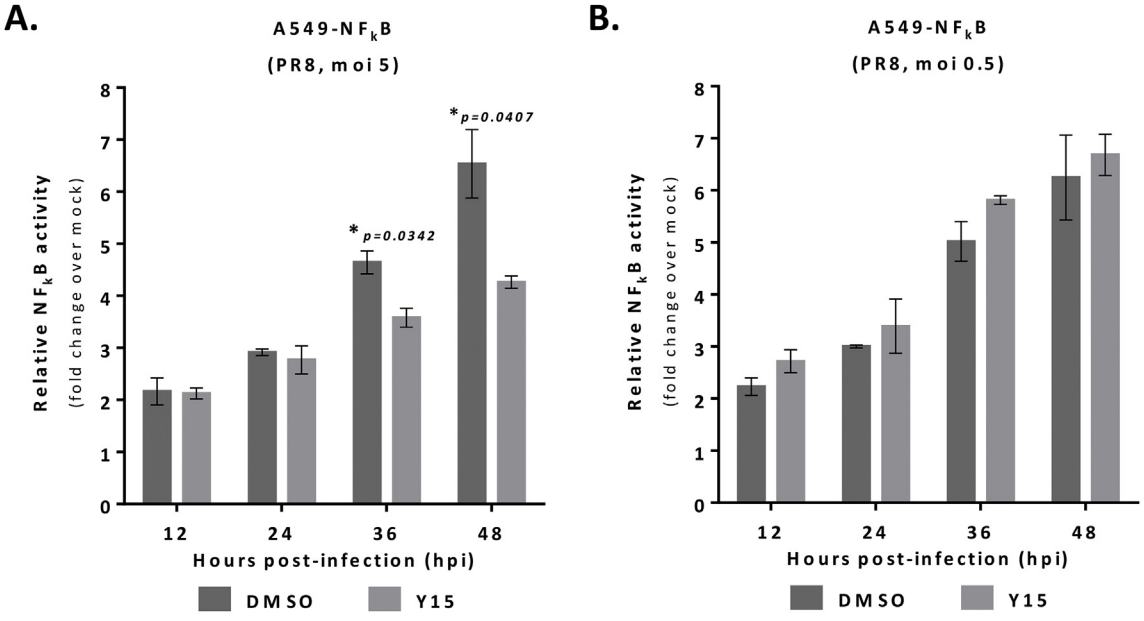

Fig. 6. Effect of Y15 on IAV-induced NFkB activation. A549-NFkB cells were infected with PR8 at moi 5 (A) or moi 0.5 (B) and supernatant was collected at indicated times. SEAP activity in the supernatant was measured using a plate reader at 630 nm. Error bars indicate standard deviation (SD) of the mean from triplicates per time-point from 3 experiments.

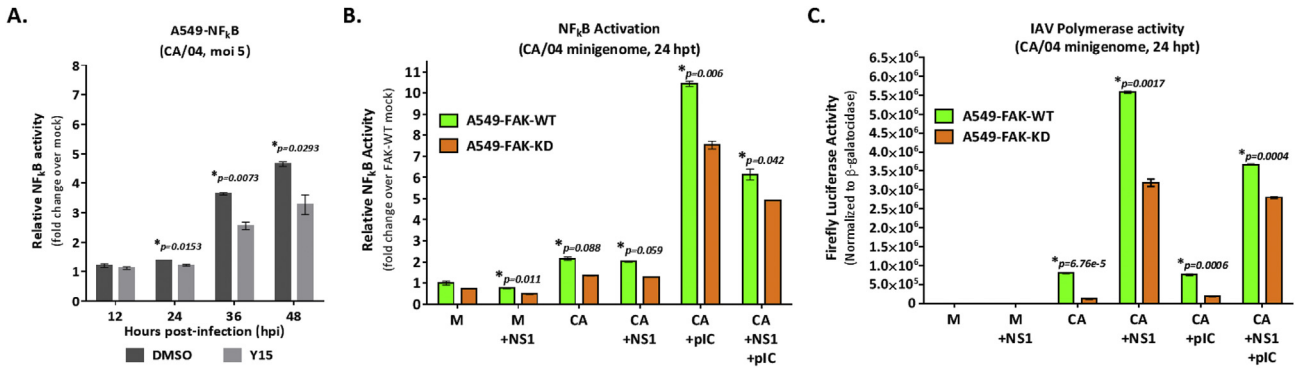

Fig. 7. Inhibiting FAK kinase activity limits IAV-induced NFkB activation. (A) A549-NFkB cells were infected with CA/04 at moi 5 and supernatant was collected at indicated times to measure SEAP activity. (B and C) A549-FAK-WT and A549-FAK-KD cells were transfected with CA/04-minigenome plasmids as well as pPOLI-358-FFluc luciferase reporter and pCMV-βgal transfection-control plasmids. Mock transfected controls were only transfected with reporter and transfection-control plasmids (M). Poly(IC) (2 μg/ml) was transfected at 6 h post transfection (+pIC). NS1 plasmid was included as indicated (+NS1). At 24 h after transfection, luciferase activity was measured and normalized to β-gal activity. Bars indicate values relative to respective A549-FAK-WT cells. Relative β-Gal activity was similar in all samples (right panel). SEAP activity (A and B) in the supernatant and luciferase expression were measured using a plate reader at 630 nm and luminometer, respectively. Error bars indicate standard deviation (SD) of the mean from triplicates per time-point from 3 experiments.

et al., 2015). Our finding that IAV-mediated NFkB is inhibited in vitro following FAK inhibition suggests cross-talk between FAK-NFkB during IAV infections. It should be noted that FAK inhibition did not reduce NFkB activity in vitro following a low moi infection. However, the implications of this is not clear for our in vivo studies as we used a very low infectious dose (50 pfu) and still observed clear differences in pro-inflammatory responses as early as 3 dpi. This suggests that dose and kinetics may not be directly comparable in vitro and in vivo in the context of FAK-dependent NFkB activation. Because NFkB activation during IAV is biphasic (Gaur et al., 2011), it is possible that FAK might only regulate one of those phases and this might be more observable at low moi's.

A major component of IAV antiviral countermeasure strategies is the viral nonstructural 1 (NS1) protein. NS1 is a multifunctional protein that regulates cytoplasmic as well as nuclear processes during IAV infections (Hale et al., 2008). In the cytoplasm, NS1 can suppress recognition of viral RNAs by RIG-I and PKR sensor proteins as well as limiting activation of IKKβ and IKKα thereby targeting both canonical and non-canonical pathways (Gao et al., 2012; Ruckle et al., 2012; Donelan et al., 2003; Gack et al., 2009). In the nucleus, IKK-mediated histone H3 phosphorylation is also disrupted by NS1 (Gao et al., 2012). Furthermore, NS1 directly interacts with PI3K which is also a FAK-interacting protein. It is intriguing to imagine an NS1-dependent regulation of FAK-mediated NFkB activation; however, our minigenome assay data indicate that the absence or presence of NS1 does not affect NFkB activation when the kinase-dead FAK mutant is expressed.

Recent studies have highlighted the importance of host kinases during in vivo IAV infections (Meineke et al., 2019). Btk inhibition in C57BL/6 (B6) mice (more resistant than D2 mice) lead to complete protection of this resistant mouse strain (Florence et al., 2018). Similarly, inhibition of GRK2 in B6 mice lead to a significant but less robust reduction in lung viral load compared to our data in susceptible D2 mice (Yanguez et al., 2018). In addition, inhibition of the lipid kinases SphK1 and SphK2 in B6 mice infected with IAV resulted in increased survival (Xia et al., 2018). Our data adds FAK to a growing list of kinases that can serve as potential targets for antiviral therapy development (Elbahesh et al., 2019). Importantly, future studies are required to identify the precise mechanism(s) of how host kinases interact with viral components and how viruses induce/hijack or suppress/evade kinase activity to replicate efficiently. Understanding these mechanisms

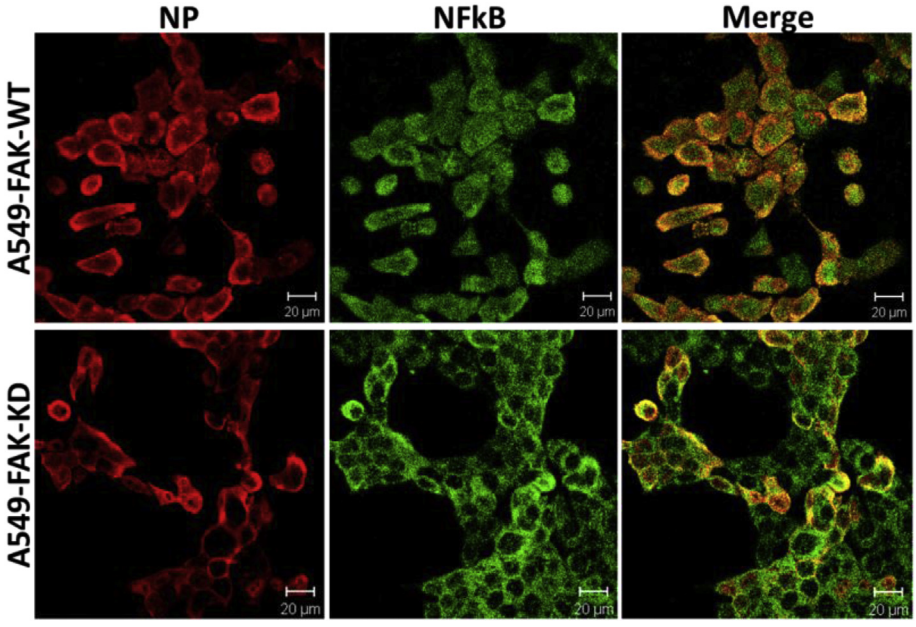

Fig. 8. FAK dependent NFkB nuclear translocation. A549 cells that overexpressed either FAK-WT or FAK-KD were IAV-infected (PR8) at moi 5 and assessed for changes in NFkB localization at 24 hpi. Viral NP and cellular NFkB (RelA/p65) were detected using anti-NP (red) and anti-NFkB-p65 (green) antibodies, respectively. Analysis was carried out by confocal microscopy using a 40× oil immersion objective (scale bars 20 μm).

may guide future anti-influenza therapies by either development of novel compounds or repurposing currently approved inhibitors/drugs.

4. Materials and methods

4.1. Ethics statement

All experimental procedures were approved by the University of Tennessee Health Science Center (UTHSC) Institutional Biosafety Committee (IBC) and Institutional Animal Care and Use Committee (IACUC) under Protocol# 15.026 and were conducted in compliance with the *Guide for the Care and Use of Laboratory Animals*. These guidelines were established by the Institute of Laboratory Animal Resources and approved by the Governing Board of the U.S. National Research Council. All experiments were performed in the UTHSC-Regional Biocontainment Laboratory which is accredited by the American Association of Laboratory Animal Science.

4.2. Cells

Madin-Darby canine kidney (MDCK) cells (from ATCC) were grown in minimal essential medium (MEM). Human alveolar lung carcinoma (A549) cells (from ATCC) were grown in F–12 K medium supplemented with 10% fetal bovine serum, 100 μg/ml streptomycin, and 100 IU/ml penicillin. A549 cells stably-expressing wild-type FAK and kinase-dead FAK (A549-FAK-WT and A549-FAK-KD, respectively) were grown in the same F–12 K media as A549 that was also supplemented with 2 mg/ml of G418. Cells were grown in a humidified 5% CO_2 incubator at 37 °C.

4.3. Viruses

Original stocks of PR8M H1N1 virus (referred to as PR8) were obtained from the strain collection at the Institute of Molecular Virology, Muenster, Germany. Pandemic H1N1 strain A/California/04/2009 (CA/04) was obtained from the St. Jude Children's Research.

Hospital repository. Viruses were propagated in the chorio-allantoic cavity of 10-day-old pathogen-free embryonated chicken eggs, aliquoted and stored at −80 °C. Virus yields were determined by a 50% tissue culture infectious dose ($TCID_{50}$) assay and plaque forming assay using MDCK cells (Reed and Muench, 1938).

4.4. Mice and infections

Inbred mouse strains DBA/2 J were obtained from Jackson Laboratories. Mice were housed under specific pathogen free conditions. For animal experiments, 8–10 week old female mice were used. Mice were treated three times with 5 mg/kg (in 20 μl 10% DMSO) Y15 (EMD Millipore) or 10%DMSO as control intranasally on −1, 0 and 1 days post-infection (dpi). For Y15 treatment, mice were anesthetized by isoflurane inhalation. For intranasal viral infections, mice were anesthetized by intra-peritoneal injection of ketamin-xylazine solution (85% NaCl (0.9%), 10% ketamine, 5% xylazine; 200 μl per 20 g body weight). Infection was performed by intranasal installation with 50 PFU of virus in 20 μl of sterile phosphate-buffered saline (PBS). Following infection, mice were monitored for mortality and moribundity including changes in body weight, scored clinical signs of illness, and mortality until 14 dpi. Additionally, mice were euthanized at days 3 and 5 for nasal cavity, tracheas and lung viral load measurements and for BAL collection. In accordance with our approved IACUC protocols (Protocol #15.026), moribund mice and/or those exhibiting > 30% body-weight loss were euthanized.

4.5. Measuring in vivo viral load

Viral load in nasal cavity, tracheal and lung tissue was determined by placing prepared tissue into 1 ml PBS containing 0.1% BSA. Tissue was subsequently homogenized using the PolyTron 2100 homogenizer. Debris was removed by centrifugation for 10 min at 1000 rpm, and aliquots of the supernatant were stored at −80 °C. Virus titers were determined as described above.

4.6. Histological staining and analysis

Lungs were prepared and immersion-fixed for 24 h in 4% buffered formaldehyde solution (pH 7.4). As negative control an uninfected tissue sample was used. Tissues were dehydrated in a series of graded ethanol and embedded in paraffin. For Hematoxylin and Eosin (H&E) staining 5 μm thick sections were used with the Hematoxylin and Eosin stain kit from ScyTek Laboratories (Logan, Utah) following the manufacturer's instructions. The incubation time with Hematoxilin was reduced to 1 min and sections were stained with Eosin for 30 s. For brightfield images slides were digitalized using Aperio Scanscope and analyzed with Aperio Imagescope software. Cellular infiltration was quantified using ImageJ Particle Measurement analysis (3 images/group). Particles were counted if they contained 3 or more pixels.

4.7. Infections in precision-cut-lung slices

Mice were sacrificed using Isoflurane under approved IACUC protocols. The trachea was cannulated, and the animals were exsanguinated by cutting the vena cava inferior. Lungs were filled with 2% low-melting agarose (SeaKem) in minimal essential medium (MEM, pH 7.2). Lungs were removed from the thoracic cavity and cooled on ice. Lung lobes were separated and afterwards cut with a Vibratome 1500 (Vibratome) into 300-μm thin slices. Lung slices were incubated in MEM containing Pen/Strep (100 U and 100 μg/ml) at 37 °C and 5% CO_2 under cell culture conditions for 2 h. The PCLS were washed with PBS and incubated overnight in IMDM contained Pen/Strep (100 U and 100 μg/ml) and Ultroser G (Pall Life Sciences) at 37 °C and 5% CO_2 under cell culture conditions. PCLS were washed with PBS and treated with 25 μM Y15 FAK inhibitor one day before the infection, day of infection and one day after infection. PCLS were infected with 1×10^4 PFU of PR8M in 100 μl infection media. After 24 and 48 h supernatant was collected for chemokine-cytokine analysis and titers.

4.8. NFkB-activation assay

We generated A549 cells (A549-NFkB) stabely expressing the NFkB-SEAP reporter. Briefly, semi-confluent (~70–80%) A549 cells (8×10^4 cells in 24-well plates) were transfected with pNiFty2-SEAP (Invivogen) using Lipofectamine LTX (Thermofisher). This plasmid encodes a secreated alkaline phosphatase (SEAP) under the control of ELAM proximal reporter and 5 NFkB repeated transcription factor binding sites.

A549-NFkB cells (10^5 cells in 24-well plates) were infected with IAV H1N1 (PR8M or CA/04) at the indicated moi and supernatants were collected at 12, 24, 36 and 48 hpi and SEAP activity was detected using QUANTI-Blue SEAP detection medium (Invivgen) according to manufacturere's protocol. Detectable SEAP activity was measured by reading at 625 nm using a BioTek Synergy2 multi-mode plate reader.

4.9. Minigenome assay for polymerase activity

Semi-confluent (~70–80%) A549 cells (8×10^4 cells in 24-well plates) were transfected using Lipofectamine LTX with a mix of plasmids encoding the PB2, PB1, PA, and NP genes from A/California/04/2009 (CA/04) strain in quantities of 0.25, 0.25, 0.25, and 0.5 μg,respectively. Where indicated, NS1 plasmid was added at 0.25 μg. The pPOLI-358-FFLuc reporter plasmid, which encodes a firefly luciferase gene under control of the viral nucleoprotein (NP) promoter (Azzeh et al., 2001; Deng et al., 2006; Hoffmann et al., 2008) (kindly provided by Megan Shaw). The pCMV-βgal plasmid (Promega)

expresses β-galactosidase, which was used for transfection normalization. For FAK inhibitor treatments, Y15 (EMD Millipore) was added at 25 μM at 24 h after transfection and cell extracts were harvested and lysed at 24 h using the M-PER mammalian protein extraction reagent (Thermo-Fisher). Luciferase levels were assayed with the One-Glo luciferase assay system (Promega). β-galactosidase activity was measure using the mammalian β-galactosidase assay (Thermo-Fisher) according to manufacturer's protocol. Luciferase luminescence and β-galactosidase absorbance were measured using a BioTek Synergy2 multi-mode plate reader.

4.10. Confocal microscopy

A549-FAK-WT and A549-FAK-KD cells on 12.5-mm coverslips in 24-well plates were infected (MOI of 5). At 24 hpi, cells were fixed in 4% paraformaldehyde at 37 °C for 20 min, permeabilized using 0.1% Triton X-100 at RT for 7 min, washed in PBS, and incubated overnight at 4 °C in blocking buffer (5% heat-inactivated horse serum in PBS). Cells were then incubated with rabbit anti-NFkB (1:150) antibody (Cell Signal) and mouse anti-NP (1:250) antibody (Millipore) diluted in blocking buffer for 1 h at room temperature, washed 3 times with PBS, and incubated for 1 h at RT with Alexa Fluor-conjugated secondary antibodies (Invitrogen) diluted in blocking buffer. Cells were then washed 3 times with PBS. Coverslips were mounted with Prolong Gold mounting medium (Invitrogen) and images were captured and analyzed by confocal microscopy.

5. Statistical analyses

Statistical analysis was performed using the PRISM (GraphPad Software, La Jolla, CA, USA) software package. Comparisons between two groups were calculated using unpaired, nonparametric Mann-Whiteny *U* test was used to determine statistical significance where appropriate. Comparisons between multiple groups (survival, weight-loss) were calculated using Mantel-Cox log-rank test.

Author contributions

HE and SB designed and performed the studies, analyzed the data, wrote and technically reviewed the manuscript.

Conflict of interest

The authors declare that they have no conflicts of interest.

Acknowledgments

We thank the UTHSC-Regional Biocontainment Laboratory staff for their technical expertise and assistance in animal experiments. We thank the UTHSC Neuroscience Institute for use of the Imaging Center. We thank Megan Shaw for providing the pPOLI358-FFLuc plasmid. This work was supported by UTHSC College of Medicine start-up funds to HE.

References

Arrese, M., Portela, A., 1996. Serine 3 is critical for phosphorylation at the N-terminal end of the nucleoprotein of influenza virus A/Victoria/3/75. J. Virol. 70 (6), 3385–3391.
Ayllon, J., Garcia-Sastre, A., 2015. The NS1 protein: a multitasking virulence factor. Curr. Top. Microbiol. Immunol. 386, 73–107.
Azzeh, M., Flick, R., Hobom, G., 2001. Functional analysis of the influenza A virus cRNA promoter and construction of an ambisense transcription system. Virology 289 (2), 400–410.
Boon, A.C., et al., 2009. Host genetic variation affects resistance to infection with a highly pathogenic H5N1 influenza A virus in mice. J. Virol. 83 (20), 10417–10426.
Bouchard, M.J., Wang, L., Schneider, R.J., 2006. Activation of focal adhesion kinase by hepatitis B virus HBx protein: multiple functions in viral replication. J. Virol. 80 (9), 4406–4414.
Bozym, R.A., et al., 2012. Focal adhesion kinase is a component of antiviral RIG-I-like receptor signaling. Cell Host Microbe 11 (2), 153–166.
Brimer, N., Wade, R., Vande Pol, S., 2014. Interactions between E6, FAK, and GIT1 at paxillin LD4 are necessary for transformation by bovine papillomavirus 1 E6. J. Virol. 88 (17), 9927–9933.
Calalb, M.B., Polte, T.R., Hanks, S.K., 1995. Tyrosine phosphorylation of focal adhesion kinase at sites in the catalytic domain regulates kinase activity: a role for Src family kinases. Mol. Cell. Biol. 15 (2), 954–963.
Chan, P.K., et al., 2012. Determinants of antiviral effectiveness in influenza virus A subtype H5N1. J. Infect. Dis. 206 (9), 1359–1366.
Chapman, N.M., et al., 2013. Focal adhesion kinase negatively regulates Lck function downstream of the T cell antigen receptor. J. Immunol. 191 (12), 6208–6221.
Cheshenko, N., et al., 2005. Focal adhesion kinase plays a pivotal role in herpes simplex virus entry. J. Biol. Chem. 280 (35), 31116–31125.
Cicchini, C., et al., 2008. TGFbeta-induced EMT requires focal adhesion kinase (FAK) signaling. Exp. Cell Res. 314 (1), 143–152.
de Jong, M.D., et al., 2005. Brief report - Oseltamivir resistance during treatment of influenza A (H5N1) infection. N. Engl. J. Med. 353 (25), 2667–2672.
Deng, T., Sharps, J.L., Brownlee, G.G., 2006. Role of the influenza virus heterotrimeric RNA polymerase complex in the initiation of replication. J. Gen. Virol. 87 (Pt 11), 3373–3377.
Dengler, L., et al., 2012. Immunization with live virus vaccine protects highly susceptible DBA/2J mice from lethal influenza A H1N1 infection. Virol. J. 9, 212.
Dengler, L., et al., 2014. Cellular changes in blood indicate severe respiratory disease during influenza infections in mice. PLoS One 9 (7), e103149.
DesRochers, B.L., et al., 2016. Residues in the PB2 and PA genes contribute to the pathogenicity of avian H7N3 influenza A virus in DBA/2 mice. Virology 494, 89–99.
Donelan, N.R., Basler, C.F., Garcia-Sastre, A., 2003. A recombinant influenza A virus expressing an RNA-binding-defective NS1 protein induces high levels of beta interferon and is attenuated in mice. J. Virol. 77 (24), 13257–13266.
Dwyer, S.F., Gao, L., Gelman, I.H., 2015. Identification of novel focal adhesion kinase substrates: role for FAK in NFkappaB signaling. Int. J. Biol. Sci. 11 (4), 404–410.
Elbahesh, H., et al., 2014. Novel roles of focal adhesion kinase in cytoplasmic entry and replication of influenza A viruses. J. Virol. 88 (12), 6714–6728.
Elbahesh, H., Bergmann, S., Russell, C.J., 2016. Focal adhesion kinase (FAK) regulates polymerase activity of multiple influenza A virus subtypes. Virology 499, 369–374.
Elbahesh, H., et al., 2019. Response modifiers: tweaking the immune response against influenza a virus. Front. Immunol. 10, 809.
Florence, J.M., et al., 2018. Inhibiting Bruton's tyrosine kinase rescues mice from lethal influenza-induced acute lung injury. Am. J. Physiol. Lung Cell Mol. Physiol. 315 (1), L52–l58.
Fouquet, B., et al., 2015. Focal adhesion kinase is involved in rabies virus infection through its interaction with viral phosphoprotein P. J. Virol. 89 (3), 1640–1651.
Gack, M.U., et al., 2009. Influenza A virus NS1 targets the ubiquitin ligase TRIM25 to evade recognition by the host viral RNA sensor RIG-I. Cell Host Microbe 5 (5), 439–449.
Gao, S., et al., 2012. Influenza A virus-encoded NS1 virulence factor protein inhibits innate immune response by targeting IKK. Cell Microbiol. 14 (12), 1849–1866.
Gaur, P., Munjhal, A., Lal, S.K., 2011. Influenza virus and cell signaling pathways. Med. Sci. Monit. 17 (6), RA148–R154.
Golubovskaya, V.M., et al., 2008. A small molecule inhibitor, 1,2,4,5-benzenetetraamine tetrahydrochloride, targeting the y397 site of focal adhesion kinase decreases tumor growth. J. Med. Chem. 51 (23), 7405–7416.
Golubovskaya, V.M., et al., 2012. A small molecule focal adhesion kinase (FAK) inhibitor, targeting Y397 site: 1-(2-hydroxyethyl)-3, 5, 7-triaza-1-azoniatricyclo [3.3.1.1(3,7)] decane; bromide effectively inhibits FAK autophosphorylation activity and decreases cancer cell viability, clonogenicity and tumor growth in vivo. Carcinogenesis 33 (5), 1004–1013.
Golubovskaya, V., et al., 2015. In vivo toxicity, metabolism and pharmacokinetic properties of FAK inhibitor 14 or Y15 (1, 2, 4, 5-benzenetetramine tetrahydrochloride). Arch. Toxicol. 89 (7), 1095–1101.
Goulet, M.L., et al., 2013. Systems analysis of a RIG-I agonist inducing broad spectrum inhibition of virus infectivity. PLoS Pathog. 9 (4), e1003298.
Hale, B.G., et al., 2008. The multifunctional NS1 protein of influenza A viruses. J. Gen. Virol. 89 (Pt 10), 2359–2376.
Hochwald, S.N., et al., 2009. A novel small molecule inhibitor of FAK decreases growth of human pancreatic cancer. Cell Cycle 8 (15), 2435–2443.
Hoffmann, H.H., Palese, P., Shaw, M.L., 2008. Modulation of influenza virus replication by alteration of sodium ion transport and protein kinase C activity. Antivir. Res. 80 (2), 124–134.
Hou, F., et al., 2011. MAVS forms functional prion-like aggregates to activate and propagate antiviral innate immune response. Cell 146 (3), 448–461.
Hsiang, T.Y., Zhou, L., Krug, R.M., 2012. Roles of the phosphorylation of specific serines and threonines in the NS1 protein of human influenza A viruses. J. Virol. 86 (19), 10370–10376.
Hu, Y.W., et al., 2013. Association between adverse clinical outcome in human disease caused by novel influenza A H7N9 virus and sustained viral shedding and emergence of antiviral resistance. Lancet 381 (9885), 2273–2279.
Hutchinson, E.C., et al., 2012. Mapping the phosphoproteome of influenza A and B viruses by mass spectrometry. PLoS Pathog. 8 (11), e1002993.
Kaminsky, P.M., et al., May 2012. Directing integrin-linked endocytosis of recombinant AAV enhances productive FAK-dependent transduction. Mol. Ther. 20 (5), 972–983.
Kim, J.I., et al., 2013. DBA/2 mouse as an animal model for anti-influenza drug efficacy evaluation. J. Microbiol. 51 (6), 866–871.
Krishnan, H.H., et al., 2006. Focal adhesion kinase is critical for entry of Kaposi's sarcoma-associated herpesvirus into target cells. J. Virol. 80 (3), 1167–1180.

Krug, R.M., 2015. Functions of the influenza A virus NS1 protein in antiviral defense. Curr Opin Virol 12, 1–6.
Kumar, N., et al., 2011a. Receptor tyrosine kinase inhibitors that block replication of influenza a and other viruses. Antimicrob. Agents Chemother. 55 (12), 5553–5559.
Kumar, N., et al., 2011b. Receptor tyrosine kinase inhibitors block multiple steps of influenza a virus replication. J. Virol. 85 (6), 2818–2827.
Kurokawa, M., et al., 1990. Inhibitory effect of protein kinase C inhibitor on the replication of influenza type A virus. J. Gen. Virol. 71 (Pt 9), 2149–2155.
Lee, S., et al., 2012. FAK is a critical regulator of neuroblastoma liver metastasis. Oncotarget 3 (12), 1576–1587.
Lim, S.T., et al., 2008. Nuclear FAK promotes cell proliferation and survival through FERM-enhanced p53 degradation. Mol. Cell 29 (1), 9–22.
Lim, S.T., et al., 2012. Nuclear-localized focal adhesion kinase regulates inflammatory VCAM-1 expression. J. Cell Biol. 197 (7), 907–919.
Maelfait, J., et al., 2012. A20 (Tnfaip3) deficiency in myeloid cells protects against influenza A virus infection. PLoS Pathog. 8 (3), e1002570.
Meineke, R., Rimmelzwaan, G.F., Elbahesh, H., 2019. Influenza virus infections and cellular kinases. Viruses 11 (2).
Mitzner, D., et al., 2009. Phosphorylation of the influenza A virus protein PB1-F2 by PKC is crucial for apoptosis promoting functions in monocytes. Cell Microbiol. 11 (10), 1502–1516.
Ni, B., et al., 2015. The involvement of FAK-PI3K-AKT-Rac1 pathway in porcine reproductive and respiratory syndrome virus entry. Biochem. Biophys. Res. Commun. 458 (2), 392–398.
Nimmerjahn, F., et al., 2004. Active NF-kappaB signalling is a prerequisite for influenza virus infection. J. Gen. Virol. 85 (Pt 8), 2347–2356.
O'Brien, S., et al., 2014. FAK inhibition with small molecule inhibitor Y15 decreases viability, clonogenicity, and cell attachment in thyroid cancer cell lines and synergizes with targeted therapeutics. Oncotarget 5 (17), 7945–7959.
O'Hara, S.D., Garcea, R.L., 2016. Murine polyomavirus cell surface receptors activate distinct signaling pathways required for infection. mBio 7 (6).
Park, S.Y., et al., 2013. Focal adhesion kinase regulates the localization and retention of pro-B cells in bone marrow microenvironments. J. Immunol. 190 (3), 1094–1102.
Pauli, E.K., et al., 2008. Influenza A virus inhibits type I IFN signaling via NF-kappaB-dependent induction of SOCS-3 expression. PLoS Pathog. 4 (11), e1000196.
Peisley, A., et al., 2013. RIG-I forms signaling-competent filaments in an ATP-dependent, ubiquitin-independent manner. Mol. Cell 51 (5), 573–583.
Peisley, A., et al., 2014. Structural basis for ubiquitin-mediated antiviral signal activation by RIG-I. Nature 509 (7498), 110–114.
Pleschka, S., et al., 2001. Influenza virus propagation is impaired by inhibition of the Raf/MEK/ERK signalling cascade. Nat. Cell Biol. 3 (3), 301–305.
Randolph, A.G., et al., 2011. Critically ill children during the 2009-2010 influenza pandemic in the United States. Pediatrics 128 (6), e1450–e1458.
Reed, L.J., Muench, H., 1938. A simple method for estimating 50% endpoints. Am. J. Hyg. 27, 493–497.
Root, C.N., et al., 2000. Entry of influenza viruses into cells is inhibited by a highly specific protein kinase C inhibitor. J. Gen. Virol. 81 (Pt 11), 2697–2705.
Ruckle, A., et al., 2012. The NS1 protein of influenza A virus blocks RIG-I-mediated activation of the noncanonical NF-kappaB pathway and p52/RelB-dependent gene expression in lung epithelial cells. J. Virol. 86 (18), 10211–10217.
Schaller, M.D., 2010. Cellular functions of FAK kinases: insight into molecular mechanisms and novel functions. J. Cell Sci. 123 (Pt 7), 1007–1013.
Shin, D.L., et al., 2015. Protection from severe influenza virus infections in mice carrying the Mx1 influenza virus resistance gene strongly depends on genetic background. J. Virol. 89 (19), 9998–10009.
Srivastava, B., et al., 2009. Host genetic background strongly influences the response to influenza a virus infections. PLoS One 4 (3), e4857.
St-Pierre, J., Ostergaard, H.L., 2013. A role for the protein tyrosine phosphatase CD45 in macrophage adhesion through the regulation of paxillin degradation. PLoS One 8 (7), e71531.
Taubenberger, J.K., Morens, D.M., 2008. The pathology of influenza virus infections. Annu. Rev. Pathol. 3, 499–522.
Tian, J., et al., 2015. Blocking the PI3K/AKT pathway enhances mammalian reovirus replication by repressing IFN-stimulated genes. Front. Microbiol. 6, 886.
Uchimura, T., et al., 2012. Analysis of cases of severe respiratory failure in children with influenza (H1N1) 2009 infection in Japan. J. Infect. Chemother. 18 (1), 59–65.
Wang, X., et al., 2000. Influenza A virus NS1 protein prevents activation of NF-kappaB and induction of alpha/beta interferon. J. Virol. 74 (24), 11566–11573.
Wang, S., et al., 2013. Tyrosine 132 phosphorylation of influenza A virus M1 protein is crucial for virus replication by controlling the nuclear import of M1. J. Virol. 87 (11), 6182–6191.
Wei, L., et al., 2006. NFkappaB negatively regulates interferon-induced gene expression and anti-influenza activity. J. Biol. Chem. 281 (17), 11678–11684.
Wurzer, W.J., et al., 2004. NF-kappaB-dependent induction of tumor necrosis factor-related apoptosis-inducing ligand (TRAIL) and Fas/FasL is crucial for efficient influenza virus propagation. J. Biol. Chem. 279 (30), 30931–30937.
Xia, C., et al., 2018. Transient inhibition of sphingosine kinases confers protection to influenza A virus infected mice. Antivir. Res. 158, 171–177.
Yanguez, E., et al., 2018. Phosphoproteomic-based kinase profiling early in influenza virus infection identifies GRK2 as antiviral drug target. Nat. Commun. 9 (1), 3679.
Zambon, M., 2014. Developments in the treatment of severe influenza: lessons from the pandemic of 2009 and new prospects for therapy. Curr. Opin. Infect. Dis. 27 (6), 560–565.
Zhang, H., et al., 2016. Efficacy of focal adhesion kinase inhibition in non-small cell lung cancer with oncogenically activated MAPK pathways. Br. J. Canc. 115 (2), 203–211.
Zheng, W., et al., 2015. Phosphorylation controls the nuclear-cytoplasmic shuttling of influenza A virus nucleoprotein. J. Virol. 89 (11), 5822–5834.